Electronic Supplementary Material (ESI) for Physical Chemistry Chemical Physics.

Supporting Information: Properties of the tetravalent actinide series in aqueous phase from a microscopic simulation self-consistent engine

Eléonor Acher,[†] Michel Masella,[¶] Valérie Vallet,[‡] and Florent Réal[*,‡]

[†]*CEA, DEN, DMRC, Univ Montpellier, Marcoule, France*

[‡]*Univ. Lille, CNRS, UMR 8523 – PhLAM – Physique des Lasers Atomes et Molécules, F-59000 Lille, France*

[¶]*Laboratoire de Biologie Structurale et Radiobiologie, Service de Bioénergétique, Biologie Structurale et Mécanismes, Institut Joliot, CEA Saclay, F-91191 Gif sur Yvette Cedex, France*

E-mail: florent.real@univ-lille.fr

Contents

List of Tables

List of Figures

1 Comments on the accuracy of DFT for total binding energies and fragment interaction energies

In the present study, we chose to compute all cluster binding energies and fragment interaction energies at the correlated MP2 level of theory, but one may question the accuracy of available functionals of the density (DFT), which depends on the simultaneous accuracies of actinide-water and water-water interactions. Réal et al.[S1] showed that GGA (BP86), a hybrid (B3LYP), and meta-GGA (M06) functionals all overestimate the Th(IV)-water interaction energy by up to $18\,\mathrm{kcal\,mol^{-1}}$. Furthermore, most functionals exhibit excessive repulsions.[S2] In Figure S1, we have compared the total binding energies and fragment interaction energies (interaction energy between a water molecule and the $An^{IV}(H_2O)_{n-1}$ cluster, computed with two GGA functionals, BLYP, PBE, one hybrid functional, PBE0, and the dispersion corrected BLYP+D3 one. All four functionals of the density overestimate the fragment interaction energies, confirming the fact that water-water repulsions are overestimated. This error is not counterbalanced by the bias in the metal-water interactions; while BLYP overestimates total binding energies, PBE, PBE0, and BLYP+D3 yield to negative deviations, the larger the hydration number the larger the deviation from MP2 energies. This confirms that currently available functionals are not accurate enough to be used for the calculations of the QM reference energies.

2 BP-P convergence

Figure S2 (a) illustrates that the five FF parameters for Th, Pu, and Bk converge after 3-5 iterations, as the training data sets is updated with sampled snapshots from classical MD simulations. The convergence of the $An-H_2O$ interaction distances and radial distribution functions as well as average coordination numbers can also be visualized on Figure S2 subsets (b) and (c).

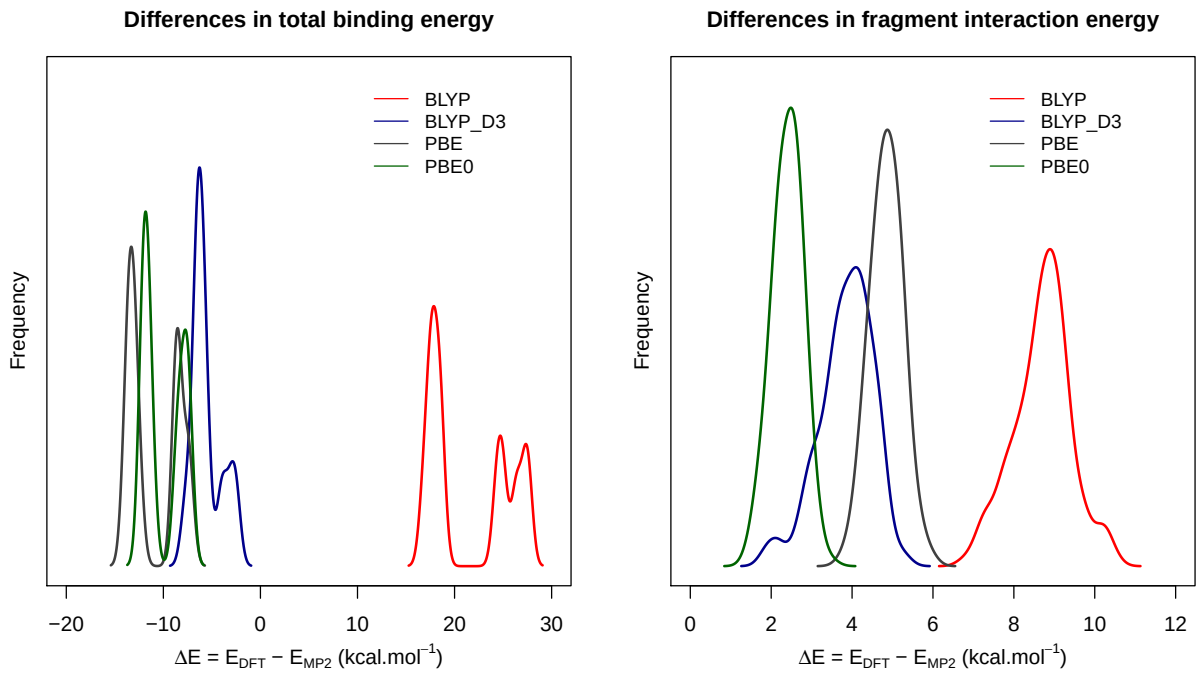

Figure S1: Differences between DFT and MP2 energies calculated on twenty clusters extracted from Th^{IV} MD for (left) total binding energy and (right) fragment interaction energies. For the total binding energies, the double peaks correspond to different coordination numbers ($Th^{IV}(H_2O)_{10}$ and $Th^{IV}(H_2O)_9$ here).

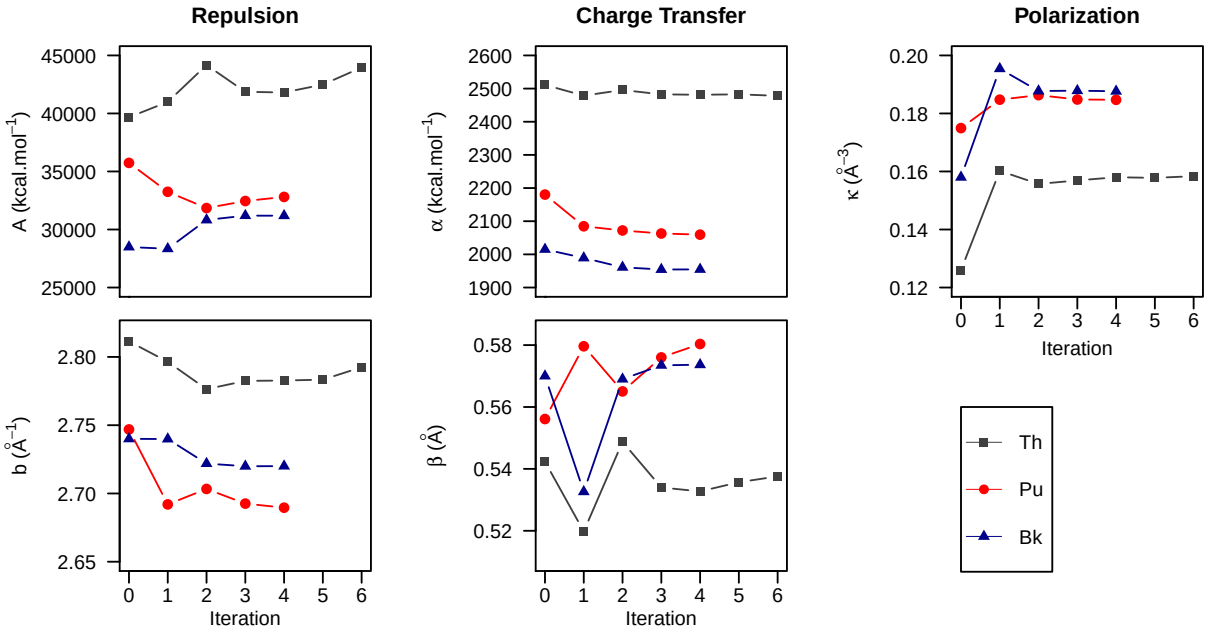

(a) Force-field parameters.

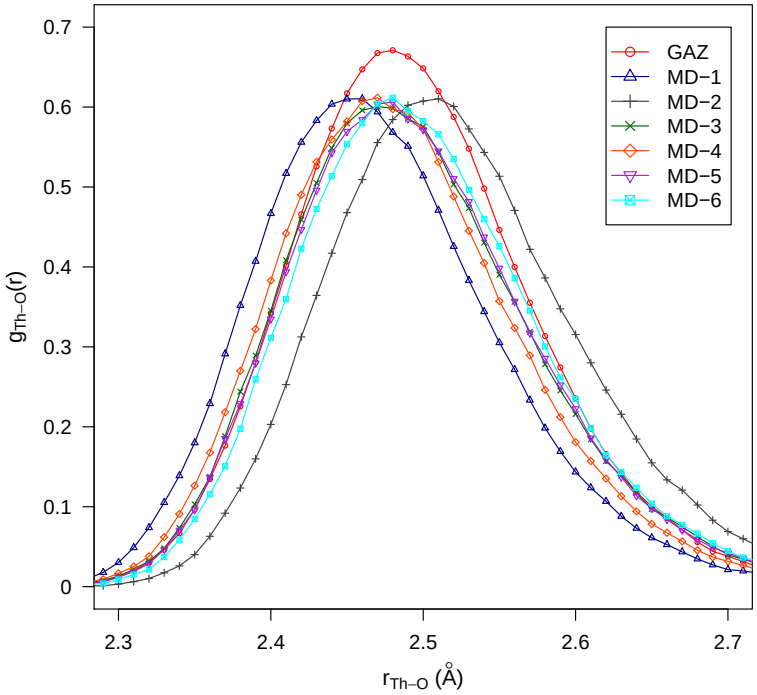

(b) Th^{IV}–O RDF.

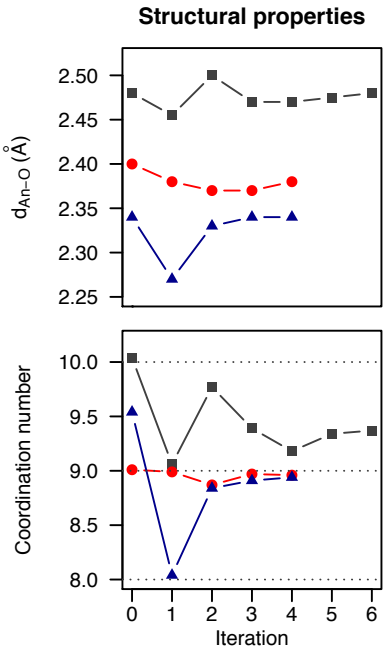

(c) Structural properties.

Figure S2: (a) Convergence of FF parameters. (b) Evolution of the Th^{IV}–O radial distribution function (RDF) along the iterations of the sampling of the solvated phase procedure *BP-P*. (c) Convergence of coordination number and An^{IV}–H_2O interaction distances for Th^{IV}, Pu^{IV} and Bk^{IV}. .

3 Final parameters

Table S1: Force-field parameters for the series of $An^{IV}-H_2O$ potentials.

	Element	A (kcal mol^{-1})	B (Å^{-1})	D^{ct} (kcal mol^{-1})	β (Å)	κ (Å^{-3})	α (Å^3)
GP-P	Th	39673	2.81	2511	0.54	0.126	1.142
	Pa	33783	2.75	2197	0.56	0.140	1.217
	U	30391	2.72	2034	0.57	0.148	1.180
	Np	26456	2.68	1715	0.59	0.146	1.063
	Pu	30692	2.76	2027	0.57	0.148	1.063
	Am	20823	2.57	1060	0.67	0.178	1.000
	Cm	19251	2.55	770	0.73	0.180	1.000
	Bk	28490	2.74	2015	0.57	0.158	1.000
	Ce	22081	2.60	1074	0.66	0.164	0.860
BP-P	Th	43960	2.792	2478	0.538	0.158	1.142
	Pa	42997	2.756	2396	0.559	0.176	1.217
	U	36135	2.704	2395	0.561	0.179	1.180
	Np	36402	2.725	2208	0.568	0.182	1.116
	Pu	32808	2.690	2060	0.580	0.185	1.063
	Am	50976	2.930	2108	0.543	0.208	1.000
	Cm	35532	2.707	2015	0.590	0.215	1.000
	Bk	31187	2.720	1955	0.574	0.188	1.000
	Ce	42891	2.867	1348	0.591	0.197	0.860

The actinide charges for Coulombic and polarization are fixed to their +4 net charge and their polarizability is either fixed to the QM values reported in the literature[S3,S4] or fixed to 1 Å^3, the latter assumption not exhibiting any significant impact on the interaction energies. Considering that the water potential parameters are fixed, only five parameters need to be adjusted with the Model-Independent Parameter Estimation (PEST) software package;[S5] namely the repulsion A_{An-i} and B_{An-i}, the charge transfer D^{ct}_{An-i} and β_{An-i} and the Thole damping one κ. The final parameters are listed in Table S1.

Table S2: Mean Residence Time (τ) in nanosecond of a water molecule in the first coordination sphere of the An^{IV}.

τ (ns)	Th	Pa	U	Np	Pu	Am	Cm	Bk	Ce
MD	0.6	0.9	1.5	1.4	1.1	0.5	0.3	1.0	0.5
Exp. S6	< 20		$\approx$185						

Table S3: Hydration free energies of the Th^{IV}-Bk^{IV} tetravalent actinide series and Ce^{IV} relative to thorium (kcal mol^{-1}), and ionic radii in Å.

	Pa	U	Np	Pu	Am	Cm	Bk	Ce	Th (absolute)
This work	-31	-58	-74	-94	-104	-121	-123	-86	
Refs. S7–S9	-17	-32	-45	-59	-69	-80	-89	-74	-1401
Ref. S10	-31	-49	-67	-85	-98	-107	-117	-79	-1400
Ref. S11		-48	-94	-82					-1457
ionic radii[S10,S12]	1.016	0.997	0.980	0.962	0.950	0.942	0.932	0.967	1.048

References

(S1) Réal, F.; Trumm, M.; Vallet, V.; Schimmelpfennig, B.; Masella, M.; Flament, J.-P. Quantum Chemical and Molecular Dynamics Study of the Coordination of Th(IV) in Aqueous Solvent. *J. Phys. Chem. B* **2010**, *114*, 15913–15924, DOI: 10.1021/jp108061s.

(S2) Gillan, M. J.; Alfè, D.; Michaelides, A. Perspective: How good is DFT for water? *J. Chem. Phys.* **2016**, *144*, 130901, DOI: 10.1063/1.4944633.

(S3) Parmar, P.; Peterson, K. A.; Clark, A. E. Static Electric Dipole Polarizabilities of Tri- and Tetravalent U, Np, and Pu Ions. *J. Phys. Chem. A* **2013**, *117*, 11874–11880, DOI: 10.1021/jp403078j.

(S4) Réal, F.; Vallet, V.; Clavaguéra, C.; Dognon, J.-P. In silico prediction of atomic static electric dipole polarizabilities of the early tetravalent actinide ions: Th^{4+} ($5f^0$), Pa^{4+} ($5f^1$), and U^{4+} ($5f^2$). *Phys. Rev. A* **2008**, *78*, 052502, DOI: 10.1103/PhysRevA.78.052502.

(S5) Doherty, J. PEST: Model-Independent Parameter Estimation and Uncertainty Analysis. 2016; see http://www.pesthomepage.org.

(S6) Farkas, I.; Grenthe, I.; Bányai, I. The Rates and Mechanisms of Water Exchange of Actinide Aqua Ions: A Variable Temperature ^{17}O NMR Study of $U(H_2O)_{10}{}^{4+}$, $UF(H_2O)_9{}^{3+}$, and $Th(H_2O)_{10}{}^{4+}$. *J. Phys. Chem. A* **2000**, *104*, 1201–1206, DOI: 10.1021/jp992934j.

(S7) Bratsch, S. G.; Lagowski, J. J. Lanthanide thermodynamic predictions. 6. Thermodynamics of gas-phase ions and revised enthalpy equations for solids at 298.15 K. *J. Phys. Chem.* **1985**, *89*, 3310–3316, DOI: 10.1021/j100261a030.

(S8) Bratsch, S. G.; Lagowski, J. J. Lanthanide thermodynamic predictions. 7. Thermodynamics of 2+, 3+, and 4+ aquo ions and standard electrode potentials at 298.15 K. *J. Phys. Chem.* **1985**, *89*, 3317–3319, DOI: 10.1021/j100261a031.

(S9) Bratsch, S. G.; Lagowski, J. J. Actinide thermodynamic predictions. 3. Thermodynamics of compounds and aquo-ions of the 2+, 3+, and 4+ oxidation states and standard electrode potentials at 298.15 K. *J. Phys. Chem.* **1986**, *90*, 307–312, DOI: 10.1021/j100274a021.

(S10) David, F. Thermodynamic properties of lanthanide and actinide ions in aqueous solution. *J. Less-Common Met.* **1986**, *121*, 27–42, DOI: 10.1016/0022-5088(86)90511-4.

(S11) David, F. H.; Vokhmin, V. Thermodynamic properties of some tri- and tetravalent actinide aquo ions. *New J. Chem.* **2003**, *27*, 1627–1632, DOI: 10.1039/B301272G.

(S12) Shannon, R. D. Revised effective ionic radii and systematic studies of interatomic distances in halides and chalcogenides. *Acta Crystallogr. A* **1976**, *32*, 751–767, DOI: 10.1107/S0567739476001551.